Heliyon 11 (2025) e41534

Contents lists available at ScienceDirect

Heliyon

journal homepage: www.cell.com/heliyon

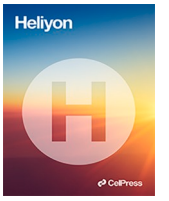

Research article

Ferroptosis genes and ST-segment elevation myocardial infarction outcomes: A predictive signature

Xing-jie Wang [a], Lei Huang [b], Min Hou [a], Jie Guo [a], Xi-ming Li [a,c,*]

[a] Clinical Laboratory, Chest Hospital, Tianjin University, Tianjin, 300222, China
[b] Heart Center, Tianjin Third Central Hospital, Tianjin, 300170, China
[c] Tianjin Key Laboratory of Cardiovascular Emergency and Critical Care, Tianjin Municipal Science and Technology Bureau, China

ARTICLE INFO

Keywords:
Myocardial infarction
Acute coronary syndrome
Ferroptosis
Prognosis
Transcriptome
Bioinformatics

ABSTRACT

Objective: The aim of this paper is to discover differentially expressed genes related to ferroptosis (DEFRGs) in patients with ST-segment elevation myocardial infarction (STEMI) and to construct a reliable prognostic signature that incorporates key DEFRGs and easily accessible clinical factors.
Methods: We did a systematic review of Gene Expression Omnibus datasets and picked datasets SE49925, GSE60993, and GSE61144 for analysis. We applied GEO2R to find DEFRGs and overlapped them among the picked datasets. We performed functional enrichment analysis to explore their biological functions. We built an optimal model with least absolute shrinkage and selection operator (LASSO) penalized Cox proportional hazards regression. We tested the clinical value of the signature with survival analysis, ROC curve, decision curve analysis and a prognostic nomogram. We also confirmed the model externally with plasma samples from our center's patients.
Results: A prognostic signature combining three overexpressed DEFRGs (*ACSL1*, *ACSL4*, *TSC22D3*) and two clinical variables (serum creatinine level, Gensini score) was established. The signature effectively classified patients into low- and high-risk groups. Survival analysis, ROC curve analysis, and DCA showed its robust predictive performance and clinical utility of the signature within two years after the onset of the disease. The external validation cohort confirmed the significant difference in major adverse cardiovascular events (MACEs) between the low- and high-risk groups.
Conclusion: This study revealed DEFRGs in patients with STEMI and developed a prognostic signature that integrates gene expression levels and clinical factors for stratifying patients and predicting the risk of MACEs.

1. Introduction

Ferroptosis is a newly discovered form of regulated cell death that depends on iron and lipid peroxidation [1]. It is involved in various pathological processes, such as cancer, neurodegeneration, and kidney injury [2–4]. One of the characteristics of ferroptosis is the peroxidation of polyunsaturated fatty acids on the cell membrane, leading to membrane rupture and cell death [5]. The occurrence of ferroptosis is regulated by multiple factors, including iron metabolism, glutamate-glutathione (GSH) cycle, antioxidant enzymes,

* Corresponding author. Clinical Laboratory, Chest Hospital, Tianjin University, 261 Taierzhuang South Road, Jinnan District, Tianjin, 300222, China.
E-mail address: ljsunlight@126.com (X.-m. Li).

https://doi.org/10.1016/j.heliyon.2024.e41534
Received 12 July 2024; Received in revised form 13 December 2024; Accepted 26 December 2024
Available online 27 December 2024

and lipid metabolism [5].

In recent years, more and more studies have shown that ferroptosis may play an important role in the pathogenesis of acute myocardial infarction (AMI) [6]. The severity and prognosis of AMI are closely related to the extent and degree of myocardial injury, which is affected by ischemia-reperfusion (I/R) injury [7]. Ferroptosis, as a novel type of cell death, may be an important component of I/R injury [6]. Some studies have found that iron overload, lipid peroxidation, and glutamate levels are significantly increased in the myocardial tissue of AMI patients, and that inhibiting ferroptosis with drugs or genes can reduce myocardial injury and improve heart function [6,8,9]. These results indicate that ferroptosis plays an important pathogenic role in AMI, and also provides new ideas and targets for AMI treatment.

ST-segment elevation myocardial infarction (STEMI) is a severe form of AMI, characterized by persistent ST-segment elevation on electrocardiogram, indicating myocardial necrosis. The prognosis of STEMI patients is influenced by multiple factors, including the degree of myocardial injury, the recovery of heart function, the occurrence of arrhythmia, etc [10]. Currently, the prognostic assessment of STEMI patients mainly relies on clinical indicators, which have limited sensitivity and specificity, and cannot fully reflect the condition and risk of STEMI patients [11]. Therefore, finding new prognostic indicators and methods is an important issue for STEMI patient management. Recently, a study reported that some genes related to ferroptosis (such as *ACSL1*) were differentially expressed in the peripheral blood of STEMI patients, and were associated with their diagnosis or myocardial protective therapy [12,13]. This suggests that integrating genes related to ferroptosis and/or clinical factors to construct a prediction model may have potential value for prognostic assessment of STEMI patients.

In this study, we will use systematic bioinformatics methods to screen for differentially expressed genes related to ferroptosis (DEFRGs) that are correlated with the prognosis of STEMI patients from the existing Gene Expression Omnibus (GEO) database of peripheral blood transcriptome data of STEMI patients. Then, we will develop a signature to predict the survival of STEMI patients based on these factors, and further evaluate its accuracy.

2. Materials and methods

2.1. Selection of the expression profile dataset

We screened the datasets that met the following criteria for further analysis: (i) datasets with plasma STEMI mRNA expression levels; (ii) discovery datasets with mRNA expression levels of STEMI patients who underwent primary percutaneous coronary intervention(PCI) and samples from healthy individuals. We excluded the datasets that had any of these conditions: (i) RNA sequencing was used for detection; (ii) The datasets did not include patients who received primary PCI; and (iii) the datasets contained data about cell types that were not present in plasma. Finally, we selected three datasets, GSE49925, GSE60993, and GSE61144, for the subsequent bioinformatics analysis. For identifying the DEFRGs between healthy control patients and STEMI patients, we used two of the smaller datasets [GSE61144: STEMI (seven samples) vs. healthy individuals (ten samples)] and [GSE60993: STEMI (seven samples) vs. healthy individuals (seven samples)] as training sets. GSE49925 with medical records and follow-up data served as a validation set for comparisons between 61 STEMI patients and 93 healthy individuals. A flowchart of the overall study design is illustrated in Fig. 1.

2.2. Identification of DEFRGs

We downloaded the raw microarray data of the two datasets GSE61144 and GSE60993 from the GEO database and used the online tool GEO2R2 (based on R package "limma") to find serum differentially expressed genes (DEGs) between STEMI patients and healthy individuals. We selected the DEGs according to $|\log2(\text{Fold Change})| > 1$ and false discovery rate (FDR) < 0.05. We obtained 1793 unique ferroptosis-related genes from the FerrDb website (http://www.zhounan.org/ferrdb/current/). Next, we identified the DEFRGs that were common to both datasets by extracting them from the DEGs. We used R package"ggplot2, VennDiagram" to draw a Venn diagram to show the intersections between DEGs and ferroptosis-related genes.

Additionally, we visually characterized the expression level of these DEFRGs by using volcano plot and difference ranking plot respectively. The expression correlation of these DEFRGs were achieved via spearman correlation and visualized with heatmaps in patients with different prognosis. The above analysis was implemented through the R package "ggplot2".

2.3. Functional and pathway enrichment analysis

We performed functional enrichment analysis to examine the biological functions of these DEFRGs, including Kyoto Encyclopedia of Genes and Genomes (KEGG) and Gene Ontology (GO) via R package "clusterProfiler". We identified the enrichment of KEGG signaling pathways and GO terms based on the criteria of FDR <0.05, followed by visualization of the top three most significant KEGG signaling pathways and GO terms via R package "ggplot2", "igraph", "ggraph".

2.4. Development of a signature combining DEFRGs

We applied the least absolute shrinkage and selection operator (LASSO) penalized Cox proportional hazards regression via R package "survival", "glmnet" to build an optimal model that integrates DEFRGs and clinical factors in the GSE49925 dataset. We selected the prognostic-related clinical variables with $P < 0.1$ as the cutoff value. Then, we computed the risk score of each STEMI patient using this formula: risk score = [Expression level of variable 1 × coefficient] + … + [Expression level of variable n ×

coefficient]. We further stratified all patients in the GSE49925 into low- and high-risk groups based on the median value of the risk score.

2.5. Clinical utility assessment of the signature

We used the median value of the risk score to split all patients in the GSE49925 into low- and high-risk groups. To validate the signature's ability to discriminate risk, we plotted the risk score distribution and the Kaplan–Meier survival curve for the two groups using the R package "survival". We also performed a time-dependent receiver operating characteristic (ROC) curve analysis (including 1-, 2-, and 3-year survival) to evaluate the signature's sensitivity and specificity using the R package "survivalROC". We also used decision curve analysis (DCA) to evaluate the net benefit of the index, which considers not only accuracy, but also the trade-off between false positives and false negatives. This part of analysis and result visualization was realized through R package "survival, stdca. R".

2.6. Construction of prognostic nomogram

We constructed a nomogram based on the model to provide a quantitative tool for predicting the survival risk of the STEMI patients. In the nomogram, each clinical variable was assigned a score and the total score was calculated by adding the scores across all the variables. We also drew calibration curves to compare the predicted and actual survival and assess the nomogram's performance. We used the R package "rms" to plot the nomogram and calibration curves.

2.7. External validation

Our hospital admitted 92 STEMI patients who underwent primary PCI between January 2020 and December 2020. The sample size was established based on the methodology outlined in our previously published works [14]. We excluded patients who had any of the following conditions: 1) cardiogenic shock; 2) history of myocardial infarction or coronary artery bypass grafting; 3) cancer or other life-threatening diseases; 4) Incomplete case documentation or missing data. We drew blood samples from the antecubital vein before PCI and kept them in EDTA tubes at −80 °C for analysis. We isolated total RNA from plasma samples with the miRNeasy Mini Kit (Qiagen, Germany) following the manufacturer's instructions. We performed reverse transcription with the High-Capacity cDNA Reverse Transcription Kit (Applied Biosystems, USA) and random primers. We estimated the relative expression levels of the target genes with the 2ˆ-ΔΔCt method.

Patients were stratified into low-risk and high-risk groups based on our median risk score value. We proactively tracked the patient cohort over a median period of 426 days without any loss to follow-up, monitoring for major adverse cardiovascular events(MACEs) such as death, repeat heart attacks, heart failure admissions, and revascularization. Kaplan-Meier survival curves and risk distribution plots were utilized to assess the prognostic value of the model.

The study follows the 1975 Declaration of Helsinki guidelines, approved by the institution's human research committee (2024LW-015, approval Date: July 4, 2024). These patients' blood samples were initially stored in the biobank with written informed consent for

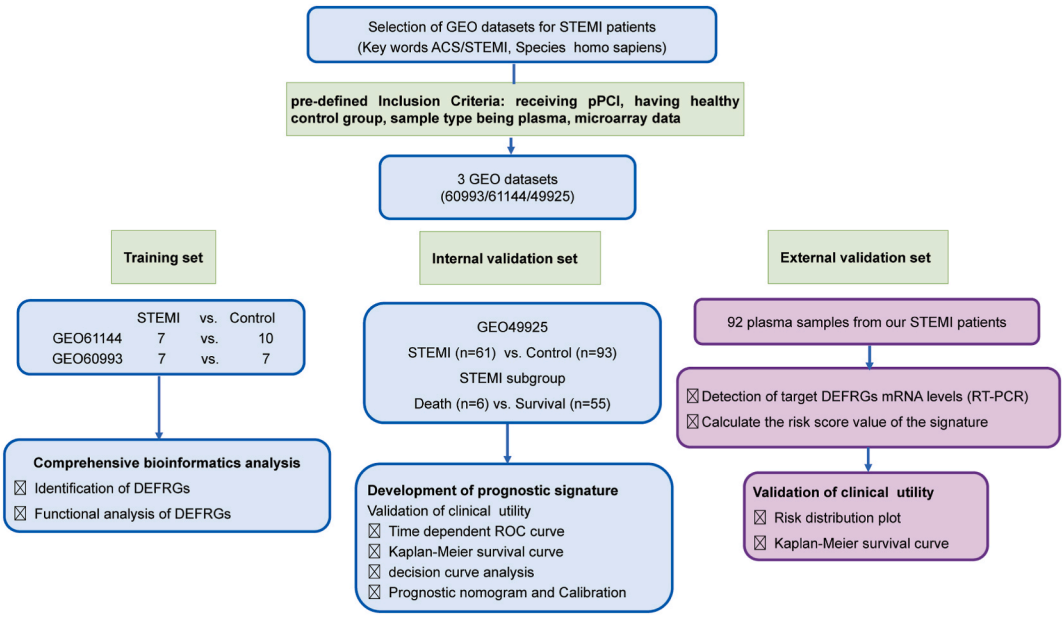

Fig. 1. Schematic flowchart of GEO dataset selection and bioinformatics analysis strategy used in this study.

future ethically approved research. Before the external validation, we informed them of the study's purpose via telephone and obtained verbal consent.

2.8. Statistical analysis

We analyzed the data using SPSS version 24.0 (SPSS Inc., Chicago, IL, United States) and R 4.2.1 (found at http://www.R-project.org, The R Foundation). We presented normal distributed quantitative data as mean standard deviation and performed *t*-tests or *t'* tests for two-group comparisons and compare the baseline demographic, clinical, and laboratory parameters. We presented quantitative data with abnormal distribution as median and interquartile ranges, and conducted Mann-Whitney *U*-tests for comparison. We presented qualitative data as frequency and composition, and applied Fisher's exact test to examine the differences in proportions between two groups. All *P* values were two-sided, and $P < 0.05$ suggested statistical significance. Schematic flowchart of GEO dataset selection and bioinformatics analysis strategy were presented in Fig. 1.

3. Results

3.1. Discovery of DEFRGs

We analyzed 14 STEMI samples and 17 normal samples from GSE60993 and GSE61144 and identified 86 DEGs. Then, we obtained 12 up-regulated DEFRGs from the DEGs (Fig. 2A, Table 1). As shown in the volcano plot (Fig. 2B) and the difference ranking plot (Fig. 2C), *ACSL1* was the most up-regulated DEFRG in the early stage of STEMI patients.

The most enriched term for biological process, cellular component, and molecular function was "fatty acid derivative biosynthetic

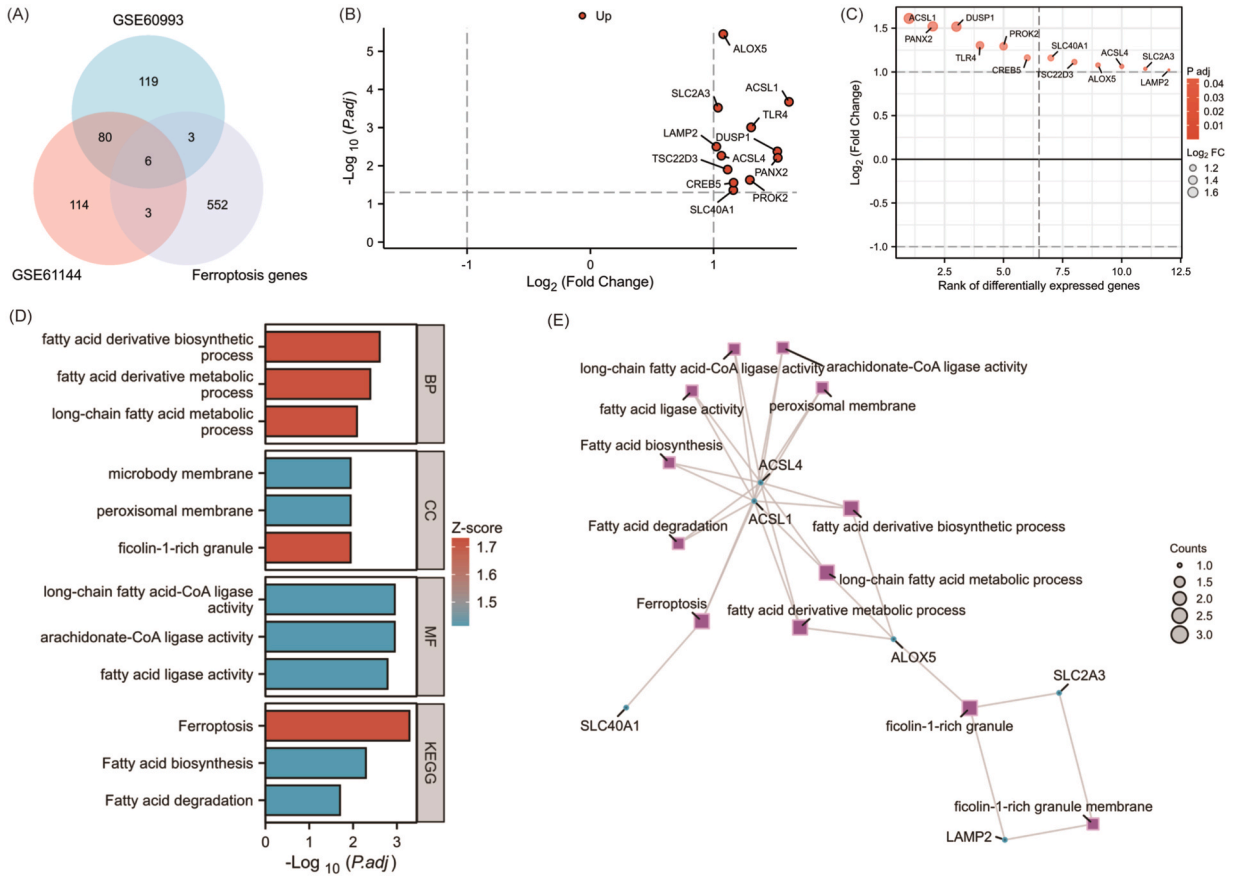

Fig. 2. Identification of DEFRGs from GSE61144 and GSE60993 microarray. (A) Venn diagram of 12 DEFRGs from the two microarray datasets. (B) The volcano plots of 12 DEFRGs in the two datasets. Red indicates genes with high levels of expression based on the criteria of $P < 0.05$ and $|\log FC| > 1.0$, respectively. (C) Ranking of the transcriptional difference among the 12 DEFRGs. DEGs differential expression genes, DEFRGs differential expression of ferroptosis-related genes. (D & E) GO enrichment and KEGG pathway analysis of 12 DEFRGs. (D) Group display of biological processes, cellular components, and molecular functions of 12 DEFRGs. (E) Network of the association between DEFRGs and GO terms and KEGG pathways. GO Gene Ontology, KEGG: Kyoto Encyclopedia of Genes and Genomes, NAD + nicotinamide adenine dinucleotide, ADP adenosine diphosphate, BP for biological process, CC for cellular component and MF for molecular function.

Table 1
12 DEFRGs were identified from GSE60993, GSE61144 microarrays for STEMI.

DEGs	Gene symbol *
Upregulated (12)	*LAMP2, TSC22D3, SLC40A1, ALOX5, SLC2A3, ACSL4, ACSL1, TLR4, DUSP1, PANX2, PROK2, CREB5*

DEFRGs, differentially expressed ferroptosis-related genes; STEMI ST-segment elevation myocardial infarction.

process", "ficolin-1-rich granule", and "arachidonate-CoA ligase activity", respectively. Functional enrichment analysis revealed that the most relevant signaling pathway to the DEFRGs was "Fatty acid biosynthesis and degradation" in the context of "ferroptosis" (Fig. 2D–Table S1). The correspondence between DEFRGs and GO terms was visualized via a network in Fig. 2E.

3.2. Development of a DEFRG prognostic signature

According to the Meta data provided, the participants were followed for a mean of 2.4 years to monitor for cardiovascular death. Among 61 patients with STEMI, 55 patients survived and six suffered cardiac death during follow-up. A principal component analysis (PCA) model for the DEFRGs was built for STEMI patients with different prognosis. The score plots of their first two principal components are shown in Fig. 3A, demonstrating a clear separation between them on the score plots, and the proportion of data variation that can be explained by the first two principal components was 78.5 % in total. In the heatmap of expression correlation, we can clearly see distinct expression profiles of the DEFRGs between groups with different prognosis (Fig. 3B). The expression correlation between the DEFRGs in the death group was significantly weakened. Moreover, we constructed a DEFRG co-expression heatmap based on an individual level, confirming that there was a significant expression correlation between DEFRGs in the survival group (Fig. 3C left), while it was significantly weakened in the death group (Fig. 3C right).

Prognosis-related parameters were identified and used to establish a prediction signature. Comparative analyses of the DEFRGs in patients with different prognosis showed that the expression levels of *ACSL1* and *ACSL4* were significantly upregulated in the death group compared to the survival group, while the inter group differences of *TSC22D3* showed a statistically significant trend (P = 0.0771) (Fig. 4A).

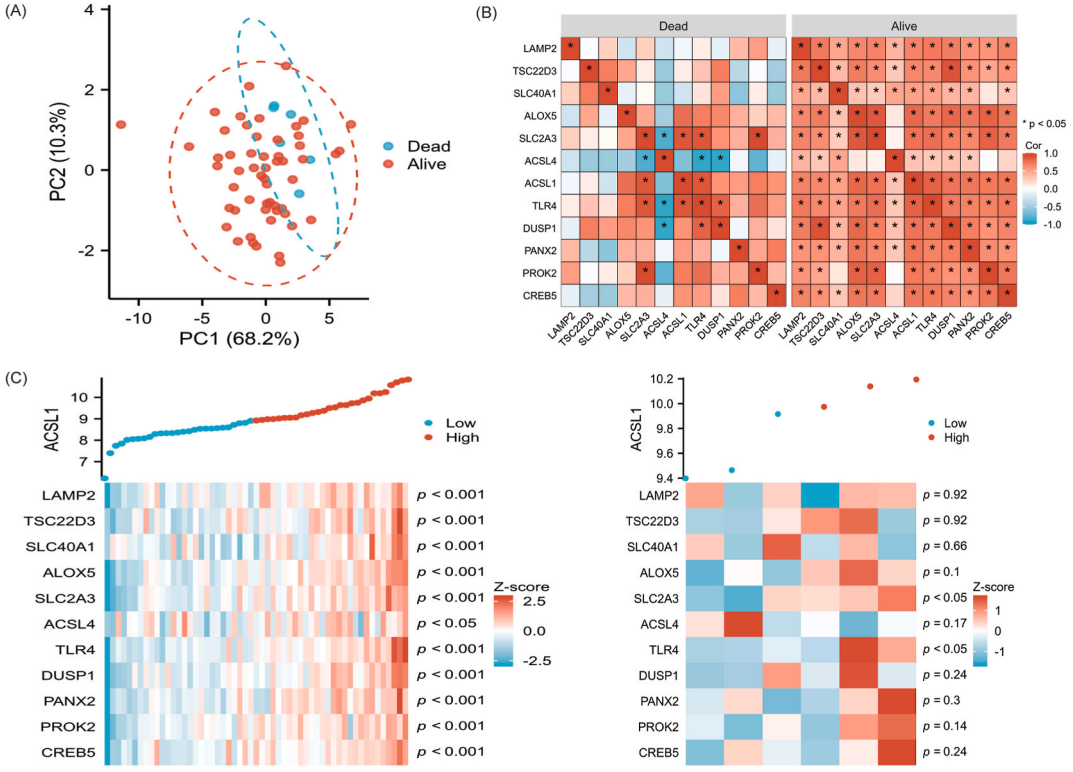

Fig. 3. The expression correlation of DEFRGs among patients who have different outcomes in the training set. (A) A principal component analysis model for the DEFRGs between groups with different outcomes. The score plots of their first two principal components were shown. (B) Expression correlation heatmap of 12 DEFRGs between different prognostic groups of GSE49925. Cor correlation coefficient. (C) Co-expression heat maps of *ACSL1* between DEFRGs based on an individual level. The correlation was significantly weakened in the death group (right) compared to the survival group (left).

Next, we incorporated all available clinical indicators (body mass index(BMI), systolic/diastolic blood pressure at admission, white blood cell count, Gensini score, high and low-density lipoprotein cholesterol, triglyceride, total cholesterol, fasting blood glucose, serum creatinine) into a LASSO penalized Cox proportional hazards regression model. This approach was particularly effective given our sample size of 61 and the necessity to streamline the number of variables. Through this analysis, BMI, serum creatinine level at admission and Gensini score were identified as key clinical factors to be included in the model (Table 2).

Given the inconsistency between variables identified by LASSO regression and multivariate Cox regression, we needed careful consideration. The hazard ratio (HR) for BMI was 0.795, suggesting a protective effect, which is paradoxical since obesity is not generally seen as protective. The GLOBAL test for the proportional hazards assumption yielded a p-value <0.05, indicating a violation. This justified our decision to exclude BMI from the final model.

After incorporating these two clinical variables along with the three ferroptosis-related genes into the predictive model, we re-evaluated the proportional hazards assumption. The GLOBAL test yielded a p-value >0.05 (Table S3), confirming that the final multivariate model met the proportional hazards assumption required for Cox regression analysis.

Thus, we developed the prognostic signature by multiplying the expression data of the key indicators by their Cox regression coefficients as follows: risk score = [Gensini score × 0.0378] + [Serum creatinine × 0.621] + [Expression level of *TSC22D3* × 3.190] + [Expression level of *ACSL4* × 13.337] + [Expression level of *ACSL1* × (−1.352)]-109.5.

3.3. The signature predicts survival of STEMI patients

We validated the signature internally using the 61 STEMI patients from GSE49925. We divided them into low- and high-risk groups based on the median value of risk score, with a threshold of 0.452. Fig. 4B shows that the death group had a much higher risk score than the survival group. The high-risk patients had a significantly lower survival than the low-risk patients (Fig. 4C).

Next, we assessed the reliability of the model using time-dependent ROC curves (Fig. 5A). The area under curve(AUC) was 0.981, 0.967, and 0.830 for 1-year, 2-year, and 3-year survival, respectively, indicating the good performance of the model in predicting short to medium term survival. A Kaplan-Meier curve also confirmed that the low-risk group had a significantly higher survival rate than the high-risk group during the follow-up period (Log-rank $P = 0.011$) (Fig. 5B). The results of DCA also showed that the signature had greater clinical net benefits than its component(s) within the first two years after the onset of STEMI (Fig. 5C), and this benefit weakened thereafter.

Last, we constructed a prognostic nomogram based on the signature (Fig. 5D, left). We performed a prognosis calibration to analyze

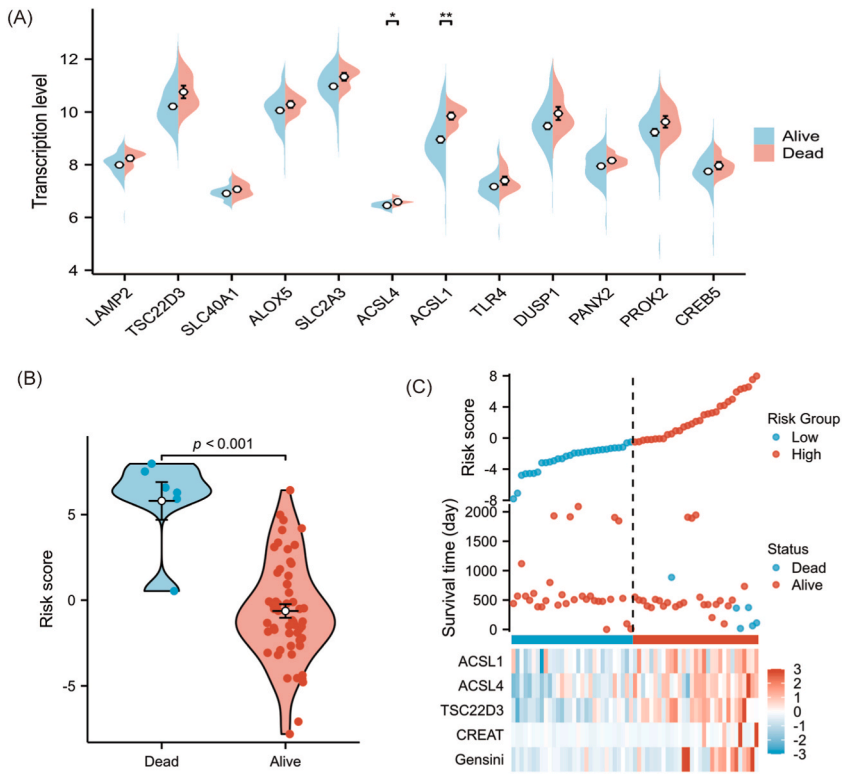

Fig. 4. GSE49925 validated the survival prediction of this signature. (A) Comparison of 12 DEFRGs in patients with different prognosis of GSE49925 (Wilcoxon rank sum test, $^*P < 0.05$). (B) Comparison of risk scores between different prognostic groups. (C) A risk distribution plot intuitively shows the significant difference of survival outcomes between the two groups with different risk stratification.

Table 2
Univariate and multivariate Cox proportional hazard regression of clinical variables in GSE49925 cohort.

Characteristics	Total(N)	Univariate analysis		Multivariate analysis	
		Hazard ratio (95 % CI)	P value	Hazard ratio (95 % CI)	P value
BMI	61	0.890 (0.778–1.017)	0.086	0.795 (0.639–0.989)	0.039
SystolicBP	61	0.986 (0.946–1.028)	0.504		
DiastolicBP	61	1.022 (0.956–1.093)	0.525		
Gensini score	61	1.012 (1.002–1.023)	0.022	1.024 (1.006–1.043)	0.007
HDL	61	1.028 (0.989–1.068)	0.165		
TRIG	61	0.982 (0.960–1.004)	0.116		
LDL	60	0.976 (0.948–1.005)	0.104		
CHOL	61	0.974 (0.945–1.004)	0.087	0.996 (0.964–1.028)	0.787
GLU	61	0.986 (0.958–1.013)	0.306		
CREAT	61	1.306 (1.113–1.532)	0.001	1.428 (1.105–1.844)	0.006
WBC	61	0.900 (0.670–1.208)	0.483		

Abbreviations: BMI Body Mass Index; SystolicBP Systolic Blood Pressure; DiastolicBP Diastolic Blood Pressure; HDL High-Density Lipoprotein Cholesterol; TRIG Triglycerides; LDL Low-Density Lipoprotein Cholesterol; CHOL Total Cholesterol; GLU Glucose; CREAT Serum Creatinine; WBC White Blood Cells.

the fit between the nomogram and the actual situation. As shown in Fig. 5D (right), the calibration curves of the nomogram showed a good agreement between predicted and actual 1- and 2-year survival in the STEMI cohort, but this accuracy modestly decreased in the third year.

3.4. External validation

We measured the transcription levels of the three genes in their peripheral blood. We calculated the risk score for each patient according to our model and divided them into low-risk and high-risk groups based on the median score. The two groups did not differ significantly in age, gender, smoking history, hypertension history, diabetes history, hyperlipidemia history, heart rate, systolic blood pressure, or diastolic blood pressure (Table 3). However, the transcription levels of the three genes, serum creatinine, and Gensini score were significantly different between the two groups ($P < 0.05$). During the prospective follow-up period (median 426 days), the low-risk group had 2 MACEs, including 1 recurrent myocardial infarction and 1 heart failure hospitalization; the high-risk group had 8 MACEs, including 1 cardiac death, 1 recurrent myocardial infarction, 5 heart failure hospitalizations, and 1 repeat revascularization. The incidence of MACEs was significantly higher in the high-risk group than in the low-risk group ($P = 0.044$). Fig. 5E indicates that the risk score of the high-risk group was skewed to the high side, while the risk score of the low-risk group was skewed to the low side. Fig. 5F shows the Kaplan-Meier survival curvesindicate that the high-risk group had a lower incidence of no-MACE events compared to the low-risk group (log-rank $P = 0.044$).

4. Discussion

STEMI is a common cardiovascular disease that requires emergency and critical care, and its pathogenesis involves the necrosis of cardiomyocytes and the activation of immune-inflammatory pathways [14,15]. In this study, we identified three DEFRGs (*ACSL1*, *ACSL4*, and *TSC22D3*) that were significantly associated with STEMI prognosis, and developed a predictive model based on these genes and two clinical indicators (serum creatinine level and Gensini score), which could effectively predict the survival risk of STEMI patients within three years after discharge. To the best of our knowledge, this is the first study to construct a prognosis model for STEMI patients using DEFRGs. Therefore, this is the main innovation and clinical utility of our research, which provides new insights into the molecular mechanisms and risk stratification of STEMI and offers new tools for improving the individualized treatment and prognosis of STEMI patients. The model was validated by multiple statistical methods, demonstrating its high accuracy and stability.

ACSL1, *ACSL4*, and *TSC22D3* are three genes involved in fatty acid metabolism and ferroptosis, which is a form of regulated cell death induced by iron-dependent lipid peroxidation [16,17]. Fatty acid metabolism plays an important role in maintaining the energy balance and homeostasis of cardiomyocytes, and its dysregulation can lead to oxidative stress, inflammation, apoptosis, and fibrosis in the myocardium [18]. Ferroptosis has been implicated in various cardiovascular diseases, such as ischemia-reperfusion injury [19], heart failure [20], and atherosclerosis [21]. We found that *ACSL1* and *ACSL4* were significantly upregulated in the death group compared to the survival group, while *TSC22D3* showed a statistically significant trend. ACSL1 and ACSL4 are two isoforms of acyl-CoA synthetase long-chain family member (ACSL), which catalyzes the conversion of free fatty acids into acyl-CoA esters for lipid synthesis or oxidation [16,22]. ACSL1 is mainly expressed in liver, adipose tissue, and skeletal muscle, while ACSL4 is mainly expressed in brain, testis, and macrophages [16]. Both ACSL1 and ACSL4 have been reported to promote ferroptosis by facilitating the incorporation of polyunsaturated fatty acids into phospholipids, which are susceptible to lipid peroxidation [23]. The upregulation of *ACSL1* and *ACSL4* may reflect the increased fatty acid metabolism and ferroptosis in STEMI patients, which may aggravate myocardial damage and inflammation, and increase the risk of adverse cardiovascular events. Therefore, *ACSL1* and *ACSL4* may be valuable prognostic biomarkers for STEMI, as well as potential therapeutic targets. TSC22D3 is a member of the TSC22 domain family of transcription factors, which regulates various biological processes such as cell proliferation, differentiation, apoptosis, and

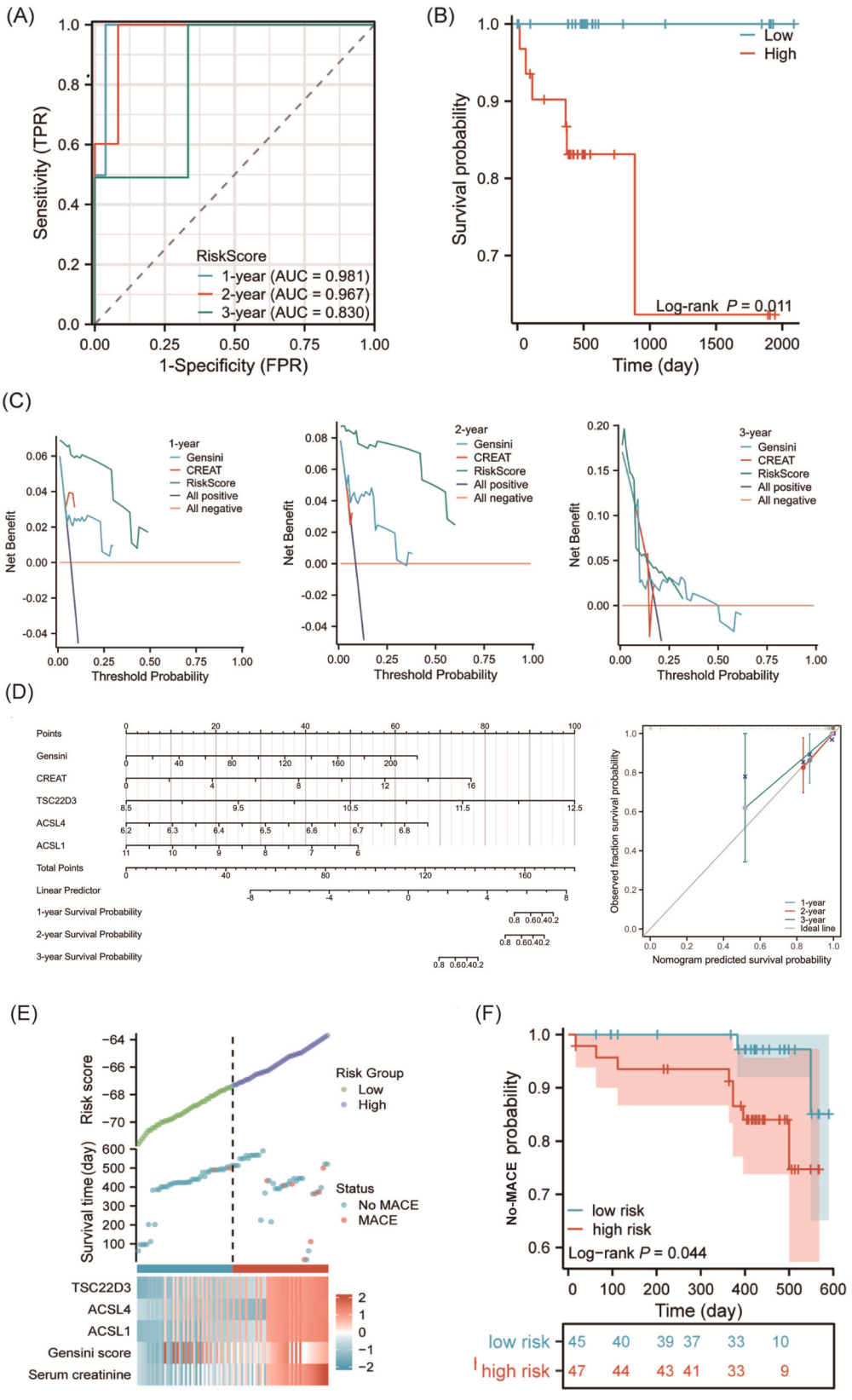

(caption on next page)

Fig. 5. The signature predicts survival of STEMI patients *in* GSE49925. (A) Time-dependent ROC curves. TPR true positive rate, FPR false positive rate. (B) Kaplan-Meier survival curves. HR hazard ratio. (C) Decision curve analysis of the constructed model at one, two and three-year of onset. (D) Nomogram for predicting 1-,2-, and 3-year survival in the entire cohort (left). And calibration curves of nomogram on consistency between predicted and observed 1-, 2- and 3-year survival in the entire cohort (right). The grey line at 45° implicated a perfect prediction, and the actual performances of our nomogram were shown in colored lines. (E & F) External validation results: (E) A risk distribution plot and (F) Kaplan-Meier survival curves showed the significant difference of survival outcomes between the two groups with different risk stratification.

Table 3
Baseline characteristics of 92 STEMI patients for external validation.

Variable	Low-risk group (n = 46)	High-risk group (n = 46)	P value
Age (years)	61.5 ± 9.8	63.2 ± 10.6	0.412
Gender (male/female)	35/11	34/12	0.810
Smoking history (yes/no)	23/23	22/24	0.835
Hypertension history (yes/no)	26/20	28/18	0.672
Diabetes history (yes/no)	12/34	14/32	0.643
Hyperlipidemia history (yes/no)	16/30	18/28	0.666
Heart rate (beats/min)	82.3 ± 12.4	84.1 ± 13.6	0.518
Systolic blood pressure (mmHg)	136.5 ± 18.7	138.2 ± 19.4	0.643
Diastolic blood pressure (mmHg)	82.4 ± 11.3	83.6 ± 12.1	0.602
Serum creatinine (mg/dL)	0.91(0.86,1.01)	1.20(1.08,1.28)	<0.001
Gensini score	36.9 ± 8.7	42.3 ± 4.6	0.016
ACSL1 ($2^{-\Delta\Delta Ct}$)	0.64(0.57,1.11)	1.33(1.13,1.39)	<0.001
ACSL4 ($2^{-\Delta\Delta Ct}$)	0.595(0.52,1.15)	1.38(1.07,1.44)	<0.001
TSC22D3 ($2^{-\Delta\Delta Ct}$)	0.69(0.63,1.14)	1.37(1.16,1.42)	<0.001

inflammation [24]. TSC22D3 has been shown to promote ferroptosis by suppressing the expression of glutathione peroxidase 4 (GPX4), a key enzyme that protects cells from lipid peroxidation [25]. The downregulation of TSC22D3 may reflect the decreased anti-ferroptotic capacity in STEMI patients, which may also contribute to myocardial injury and inflammation [26]. Therefore, *TSC22D3* may also be a valuable prognostic biomarker for STEMI, as well as a potential therapeutic target.

The clinical applicability of our predictive signature is a critical aspect of this study. Our model integrates differentially expressed DEFRGs with easily accessible clinical factors, providing a comprehensive tool for stratifying STEMI patients and predicting their survival risk. This approach offers several advantages over existing prognostic tools. Firstly, traditional risk stratification methods, such as the TIMI risk score and the GRACE risk model, rely on clinical predictors and large databases of patient outcomes. While these tools are valuable, they do not incorporate gene expression data, which can offer deeper insights into the molecular mechanisms underlying STEMI. Our model bridges this gap by combining genetic and clinical information, potentially enhancing the accuracy and specificity of risk prediction. Secondly, we of the accuracy and stability of the predictive model we constructed our predictive signature has demonstrated robust performance in both internal and external validation cohorts via performing multidimensional validation. In the development phase of the model, risk factor distribution plot, Kaplan-Meier survival analysis, time-dependent ROC curves analysis, calibration curve analysis to a prognostic nomogram, and decision curve analysis all indicate that our model effectively classifies patients into low- and high-risk groups during the first 2-year follow-up period, with significant differences in survival outcomes. This suggests that our model could be a valuable addition to the current prognostic tools used in clinical practice. In our external validation cohort, the relative expression levels of the three genesremained significantly different between the low-risk and high-risk groups, consistent with our previous bioinformatics analysis. Notably, the gene transcription levels measured by microarray and RT-PCR were inherently different types of data, with distinct ranges and units. To address this, weutilized RT-PCR data to calculate individual risk scores, and established a new risk stratification threshold based on the cohort's overall risk scores. Our findings affirmed that this model could effectively distinguish patients with varying prognostic risk levels. Although the Kaplan-Meier survival curve did not show a significant difference in the incidence of MACEs between the two groups, the *p*-value was close to 0.05. This suggests that the lack of statistical significance may be due to the limited sample size of the validation cohort, indicating that threshold selection for the grouping requires further optimization.

Moreover, the integration of DEFRGs into the prognostic model provides a novel approach to understanding the pathophysiology of STEMI. By identifying genes associated with ferroptosis, a form of regulated cell death, our model offers insights into potential therapeutic targets and personalized treatment strategies. This study has some limits. One of the major limitations is the small sample size and short follow-up time of the external validation cohort, which might have resulted in insufficient statistical power to detect a significant difference in survival between different risk groups. We observed a significant difference in the incidence of MACEs between the two groups, and our model performed well in various other metrics. Therefore, we believe that our sample size was adequate for the purpose of our study, and that our results were reliable and generalizable. Future studies should use larger sample sizes and longer follow-up times to validate our model, as well as explore more potential prognostic factors.

5. Conclusion

Our study presents a promising predictive signature that combines genetic and clinical factors to improve the risk stratification of

STEMI patients. The incorporation of DEFRGs (*ACSL1*, *ACSL4*, and *TSC22D3*) and the validation of our model highlight its potential clinical utility and value. Future studies should focus on further refining and implementing this model in clinical settings to enhance patient care and outcomes.

CRediT authorship contribution statement

Xing-jie Wang: Writing – review & editing, Writing – original draft, Visualization, Validation, Software, Resources, Project administration, Methodology, Investigation, Formal analysis, Data curation. **Lei Huang:** Writing – review & editing, Writing – original draft, Visualization, Supervision, Software, Project administration, Methodology, Investigation, Formal analysis, Data curation, Conceptualization. **Min Hou:** Writing – review & editing, Validation, Project administration, Methodology, Investigation, Data curation, Conceptualization. **Jie Guo:** Writing – review & editing, Validation, Software, Project administration, Methodology, Investigation. **Xi-ming Li:** Writing – review & editing, Writing – original draft, Supervision, Project administration, Methodology, Investigation, Funding acquisition, Formal analysis, Data curation, Conceptualization.

Ethics statement

This study was reviewed and approved by the ethical review boards of Tianjin Chest Hospital (approval number: 2024LW-015) on July 4, 2024. The research involving human subjects was conducted in compliance with the Code of Ethics of the World Medical Association (Declaration of Helsinki). Written informed consent was obtained from all patients for participation in the study and publication of their data.

Data availability statement

The datasets generated and/or analyzed during the current study are available in the GEO repository (https://www.ncbi.nlm.nih.gov/geo/query/acc.cgi?acc=GSE60993, https://www.ncbi.nlm.nih.gov/geo/query/acc.cgi?acc=GSE61144, https://www.ncbi.nlm.nih.gov/geo/query/acc.cgi?acc=GSE49925)

Declaration of competing interest

The authors declare that they have no known competing financial interests or personal relationships that could have appeared to influence the work reported in this paper.

Acknowledgements

This research was supported by the grant from Tianjin Key Medical Discipline (Specialty) Construction Project (NO.TJYXZDXK-055B), Tianjin Science and Technology Program of China (21JCYBJC01590) and research project of Tianjin Municipal Health Commission (2023013).

Appendix A. Supplementary data

Supplementary data to this article can be found online at https://doi.org/10.1016/j.heliyon.2024.e41534.

References

[1] Y. Wang, J. Wu, Ferroptosis: a new strategy for cardiovascular disease, Front Cardiovasc Med 10 (2023) 1241282.
[2] Q. Wang, J. Sun, T. Chen, S. Song, Y. Hou, L. Feng, et al., Ferroptosis, pyroptosis, and cuproptosis in alzheimer's disease, ACS Chem. Neurosci. 14 (19) (2023) 3564–3587.
[3] S. Li, R. Wang, Y. Wang, Y. Liu, Y. Qiao, P. Li, et al., Ferroptosis: a new insight for treatment of acute kidney injury, Front. Pharmacol. 13 (2022) 1065867.
[4] Y.C. Liu, Y.T. Gong, Q.Y. Sun, B. Wang, Y. Yan, Y.X. Chen, et al., Ferritinophagy induced ferroptosis in the management of cancer, Cell. Oncol. 47 (1) (2023) 19–35.
[5] S. Li, P. Huang, F. Lai, T. Zhang, J. Guan, H. Wan, et al., Mechanisms of ferritinophagy and ferroptosis in diseases, Mol. Neurobiol. 61 (3) (2023) 1605–1626.
[6] X. Han, J. Zhang, J. Liu, H. Wang, F. Du, X. Zeng, et al., Targeting ferroptosis: a novel insight against myocardial infarction and ischemia-reperfusion injuries, Apoptosis 28 (1–2) (2023) 108–123.
[7] H. Zhang, H. Hu, C. Zhai, L. Jing, H. Tian, Cardioprotective strategies after ischemia-reperfusion injury, Am. J. Cardiovasc. Drugs 24 (1) (2023) 5–18.
[8] Q. Yu, N. Zhang, X. Gan, L. Chen, R. Wang, R. Liang, et al., EGCG attenuated acute myocardial infarction by inhibiting ferroptosis via miR-450b-5p/ACSL4 axis, Phytomedicine 119 (2023) 154999.
[9] J. Laukaitiene, G. Gujyte, E. Kadusevicius, Cardiomyocyte damage: ferroptosis relation to ischemia-reperfusion injury and future treatment options, Int. J. Mol. Sci. 24 (16) (2023).
[10] G.R. Shamaki, I. Safiriyu, O. Kesiena, C. Mbachi, M. Anyanwu, S. Zahid, et al., Prevalence and outcomes in STEMI patients without standard modifiable cardiovascular risk factors: a national inpatient sample analysis, Curr. Probl. Cardiol. 47 (11) (2022) 101343.
[11] I. Ramasamy, Biochemical markers in acute coronary syndrome, Clin. Chim. Acta 412 (15–16) (2011) 1279–1296.
[12] Z.Y. Liu, F. Liu, Y. Cao, S.L. Peng, H.W. Pan, X.Q. Hong, et al., ACSL1, CH25H, GPCPD1, and PLA2G12A as the potential lipid-related diagnostic biomarkers of acute myocardial infarction, Aging 15 (5) (2023) 1394–1411.

[13] J. Wu, H. Cai, Z. Lei, C. Li, Y. Hu, T. Zhang, et al., Expression pattern and diagnostic value of ferroptosis-related genes in acute myocardial infarction, Front Cardiovasc Med 9 (2022) 993592.
[14] W. Gao, X.Y. Wang, X.J. Wang, L. Huang, An integrated signature of clinical metrics and immune-related genes as a prognostic indicator for ST-segment elevation myocardial infarction patient survival, Heliyon 10 (10) (2024) e31247.
[15] Z. Peng, H. Chen, M. Wang, Identification of the biological processes, immune cell landscape, and hub genes shared by acute anaphylaxis and ST-segment elevation myocardial infarction, Front. Pharmacol. 14 (2023) 1211332.
[16] J. Quan, A.M. Bode, X. Luo, ACSL family: the regulatory mechanisms and therapeutic implications in cancer, Eur. J. Pharmacol. 909 (2021) 174397.
[17] J. Ma, C. Li, T. Liu, L. Zhang, X. Wen, X. Liu, et al., Identification of markers for diagnosis and treatment of diabetic kidney disease based on the ferroptosis and immune, Oxid. Med. Cell. Longev. 2022 (2022) 9957172.
[18] T. Yamamoto, M. Sano, Deranged myocardial fatty acid metabolism in heart failure, Int. J. Mol. Sci. 23 (2) (2022).
[19] R. Wang, X. Chen, X. Li, K. Wang, Molecular therapy of cardiac ischemia-reperfusion injury based on mitochondria and ferroptosis, J. Mol. Med. (Berl.) 101 (9) (2023) 1059–1071.
[20] K. Zhang, X.M. Tian, W. Li, L.Y. Hao, Ferroptosis in cardiac hypertrophy and heart failure, Biomed. Pharmacother. 168 (2023) 115765.
[21] X. Wan, H. Zhang, J. Tian, P. Hao, L. Liu, Y. Zhou, et al., The chains of ferroptosis interact in the whole progression of atherosclerosis, J. Inflamm. Res. 16 (2023) 4575–4592.
[22] T. Zhang, W. Deng, Y. Deng, Y. Liu, S. Xiao, Y. Luo, et al., Mechanisms of ferroptosis regulating oxidative stress and energy metabolism in myocardial ischemia-reperfusion injury and a novel perspective of natural plant active ingredients for its treatment, Biomed. Pharmacother. 165 (2023) 114706.
[23] H. Yuan, X. Li, X. Zhang, R. Kang, D. Tang, Identification of ACSL4 as a biomarker and contributor of ferroptosis, Biochem. Biophys. Res. Commun. 478 (3) (2016) 1338–1343.
[24] E. Ayroldi, M.G. Petrillo, M.C. Marchetti, L. Cannarile, S. Ronchetti, E. Ricci, et al., Long glucocorticoid-induced leucine zipper regulates human thyroid cancer cell proliferation, Cell Death Dis. 9 (3) (2018) 305.
[25] X.D. Zhang, Z.Y. Liu, M.S. Wang, Y.X. Guo, X.K. Wang, K. Luo, et al., Mechanisms and regulations of ferroptosis, Front. Immunol. 14 (2023) 1269451.
[26] R.T. Hahn, J. Hoppstädter, K. Hirschfelder, N. Hachenthal, B. Diesel, S.M. Kessler, et al., Downregulation of the glucocorticoid-induced leucine zipper (GILZ) promotes vascular inflammation, Atherosclerosis 234 (2) (2014) 391–400.